MOVPE Growth of High Quality AlN Layers and Effects of Si-doping

Sarad Bahadur Thapa

High quality undoped AlN layers were grown by LP–MOVPE by using optimized growth conditions for nucleation and bulk layers. AFM measurements revealed a rms surface roughness of 0.2 nm with a hexagonal pit density well below 10^5 cm^{-2}. The FWHM of HRXRD for the (002) and (114) reflections are 59 and 390 arcsec, respectively. This excellent quality of our AlN layers is further confirmed by low temperature CL spectra with a FWHM of 10 meV. Furthermore, we have studied the effects of Si incorporation on the structural and spectroscopic properties of AlN layers. We found that the surface quality deteriorates with increasing Si concentrations. Surprisingly, the HRXRD (002) peak is much narrower for our Si doped samples. With increasing Si concentrations up to 10^{19} cm^{-3}, both reflections, (002) and (114), get broader. However, their width decreases again for even higher concentrations, which is accompanied by the development of cracks. Accordingly, HRXRD and low temperature CL measurements show that the in-plane tensile stress of our Si-doped layers increases up to Si concentrations of 10^{19} cm^{-3}, whereas a stress release is observed for higher concentrations.

1. Introduction

Among the group III nitride materials, aluminum nitride (AlN) has attracted much attention due to its large direct bandgap (approx. 6.0 eV) and outstanding thermal and chemical stability. It has a wide application perspective especially in the area of high–power high–temperature electronic devices. Due to the piezoelectric and electromechanical coupling properties, high propagation rate, and low transmission loss, AlN can also be used in various types of acoustic devices [1, 2]. Recently, a report of an LED with a wavelength of 210 nm [3] has demonstrated the strong possibility of a promising application of this material in the field of optoelectronics in the days ahead. Meantime, many groups have been using AlN as a template for the fabrication of UV devices [4, 5]. Furthermore, AlN/GaN superlattice structures can be used in optical devices operating at telecommunication wavelengths by exploiting intersubband transitions between bound quantum well states [6, 7]. However, the growth of high quality AlN, as required for device fabrication, is still a big challenge. Especially the proper doping of AlN layers to obtain electrical conduction as a device performance quality remains to be a key issue for the nitride researchers.

We have previously reported the influence of various growth parameters on the structural and spectroscopic properties of AlN bulk layers [8]. In this report, we present the results of a high quality AlN bulk layer after further optimization of the nucleation layer and subsequent stages. In addition, we investigated the incorporation of Si donors and their influence on the properties of the AlN crystal quality.

2. Experiment

Undoped layers of AlN, approximately 500 nm thick, were grown on c–plane sapphire substrates in an AIXTRON AIX 200 RF LP–MOVPE system by using trimethylaluminum (TMAl) and NH_3 as precursors and H_2 as a carrier gas in N_2 and H_2 atmosphere. To achieve a high quality AlN layer, the growth process was optimized by dividing it into 3 parts, namely, 1. Oxygen doped AlN nucleation layer, 2. Stage between nucleation and AlN bulk layer, and 3. AlN bulk layer.

During the optimization of the nucleation layer, the growth conditions of subsequently deposited AlN bulk layers, as given in Table 3, were kept constant. Oxygen from t–Butanol, used as liquid source in conventional bubbler configuration, was supplied in the form of pulses (2 sec on, 28 sec off) whereas TMAl and NH_3 were turned on throughout the nucleation process [9]. As we need a very small amount of oxygen doping during the nucleation layer growth, the pulsed supply could be an effective method to precisely control the amount. This method offers good controllability as we can vary the pulse width and period in addition to the mass flows. The range of growth parameters of the nucleation layer is given in Table 3. After the growth of the nucleation layer, the reactor temperature was increased to the bulk layer growth temperature under NH_3 atmosphere.

Table 3: Growth conditions of subsequently deposited AlN bulk layer after nucleation layer and range of growth parameters for the nucleation layer optimization.

Growth Parameters	Subsequently grown AlN bulk layer	Range for nucleation layer optimization
Growth Pressure	35 mbar	35 - 100 mbar
Growth Temperature	1150°C	820 - 930°C
V–III Ratio	2000	500 - 18000
N_2–H_2 Ratio	1.3	0.8 - 4.0
Total Flow	2500 sccm	1500 - 5000 sccm

Three different procedures were implemented at the stage between the nucleation and bulk layer growths. Those were: a) Continuous growth of AlN bulk layer after the nucleation layer during the ramping up of temperature, b) Thermal annealing of nucleation layer under NH_3 before bulk layer growth, and c) Cooling the nucleation layer down to 400°C under NH_3 atmosphere and ramping the reactor temperature up to the bulk layer growth temperature followed by a short pre-flow of NH_3 before bulk layer growth. Moreover, the growth temperature of the bulk layer was increased from 1150°C to 1190°C while keeping the other growth parameters constant as given in Table 3.

Si doping was performed by typically depositing a 250 nm thick Si-doped AlN layer on a 250 nm thick optimized undoped AlN buffer layer at the growth temperature of 1150°C. Si was incorporated by using silane (SiH_4) as a Si source through a double dilution configuration of massflow controllers. The basic growth conditions of the Si–doped layers were

similar to those of the undoped buffer layers. The Si concentration was extrapolated from our growth parameters using other AlN samples as reference which had been measured by secondary ion mass spectroscopy (SIMS) [10].

The surface quality was analyzed by using atomic force microscopy (AFM). High–resolution X–ray diffraction (HRXRD) rocking curve measurements for the symmetric and asymmetric reflections were carried out to examine the crystal quality of bulk AlN epitaxial layers. Low temperature (T=10 K) cathodoluminescence (CL) provided information about the spectroscopic properties.

3. Results and Discussions

3.1 Undoped AlN layer

Continuing our previous studies described in [11], we have determined the optimized growth parameters for a nucleation layer as given in Table 4.

Table 4: Optimized growth parameters for the nucleation layer.

Growth Parameters	Optimized value
Growth Pressure	70 mbar
Growth Temperature	870°C
V–III Ratio	2500
N_2–H_2 Ratio	1.9
Total Flow	2000 sccm

We observed that the amount of oxygen supplied in the nucleation layer is one of the critical parameters for the surface and crystal quality of AlN. Both the rms surface roughness and FWHM of HRXRD for the (002) reflection of the AlN bulk layers could be minimized when the supply of oxygen was 5 pulses in comparison to the nucleation layer without and with the supply of larger number of oxygen pulses (Fig. 1(left)). The AlN quality is further improved by 2 min extended growth of the AlN nucleation layer without oxygen doping as demonstrated in Fig. 1(right). However, longer times produced a negative effect on both the surface and crystal quality. With these results, we confirmed that oxygen doping is needed just at the beginning of the nucleation layer growth. The total thickness of the nucleation layer should be approximately 30 nm to obtain a high quality AlN layer where only the first part is doped with oxygen.

In a next step, we studied the influence of various processes carried out at the stage between nucleation and bulk layer growth on the quality of AlN. The continuous growth of AlN after the nucleation layer during the ramping up of temperature decreased both, the surface and crystal quality. Though the thermal annealing of the nucleation layer under NH_3 before the growth of the bulk layer improved the crystal quality, it had very bad effect on the surface quality due to the strong decomposition of the nucleation layer.

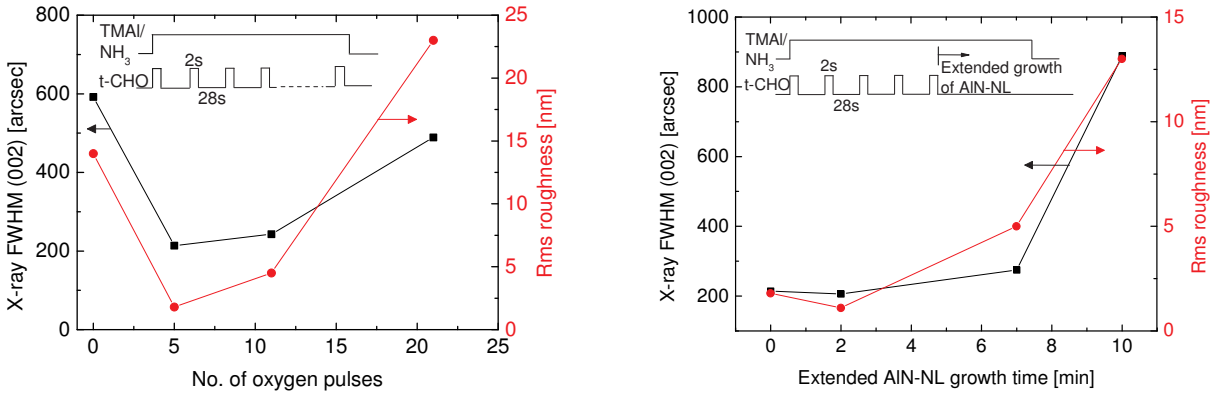

Fig. 1: FWHM of HRXRD for the (002) reflection and rms surface roughness of AlN bulk layers: Plots for different numbers of oxygen pulses supplied during the nucleation layer growth (left), extended growth of the AlN nucleation layer after the supply of 5 pulses of oxygen at the beginning of the nucleation process (right).

However, among the three procedures described in section 2, cooling down of the nucleation layer till 400°C under NH_3 atmosphere and ramping the reactor temperature to the bulk layer growth temperature followed by a short pre–flow of NH_3 enhanced both the surface and crystal quality of AlN further. Cooling down of the nucleation layer might relax the stress induced by thermal mismatch. Hence, further effect of thermal strain on subsequently grown AlN bulk layer was minimized with this procedure. The short pre–flow of NH_3 before the growth of the bulk layer may assist the re–crystallization and further coalescence of AlN islands of the nucleation layer at high temperature which in effect transforms the 3D growth mode of the nucleation layer to 2D growth of the bulk layer.

After the optimization of these initial parts of our growth procedure, we obtained high quality AlN as given in Table 5(a). Further rise of the bulk layer growth temperature from 1150°C to 1190°C finally resulted in a very high quality of AlN (Table 5(b)). The hexagonal pit density on the surface was significantly reduced to less than $10^5\,\mathrm{cm}^{-2}$. Figure 2 shows an AFM image of an atomically flat layer with a measured rms value of the surface roughness of 0.2 nm. The FWHM of the X-ray rocking curve for the (002) and (114) reflections are 59 and 390 arcsec, respectively. These excellent data were further confirmed by a band edge excitonic emission with a FWHM of 10 meV (Fig. 3). The LO phonon replica confirm the good optical quality of the bulk AlN epitaxial layers.

3.2 Si-doped AlN layer

In order to influence the electrical properties of our AlN layers, we investigated Si doping. Similar as reported by Ive et al.[12], we found that it has an adverse effect on the surface quality of AlN. As shown in Fig. 4, we observed the formation of a large number of pits on the surface attributed to the effect of Si doping. Moreover, the Si incorporation has shown a remarkable impact on the crystal quality of AlN [13]. Surprisingly, the HRXRD (002) peak is much narrower for our Si doped samples as compared to their undoped counterparts whereas the (114) peak is slightly broader. For both, (002) and

Table 5: Result of the optimized AlN bulk layers.

Parameters	Growth at 1150°C (a)	Growth at 1190°C (b)
Rms surface roughness	0.4 nm	0.2 nm
Hexagonal pit density	$\approx 10^7\,\mathrm{cm}^{-2}$	$< 10^5\,\mathrm{cm}^{-2}$
FWHM of HRXRD (002) reflection	200 arcsec	59 arcsec
FWHM of HRXRD (114) reflection	600 arcsec	390 arcsec
FWHM of low temp. CL peak	$\approx$ 20 meV	$\approx$ 10 meV

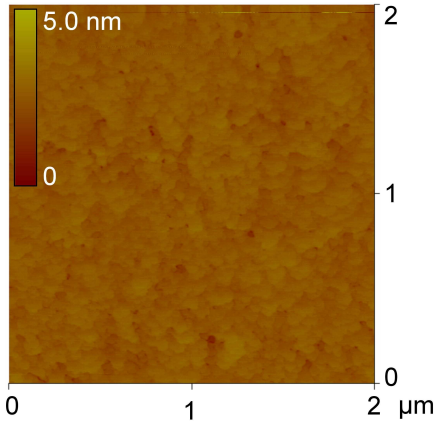

Fig. 2: AFM image of the optimized AlN bulk layer grown at 1190°C.

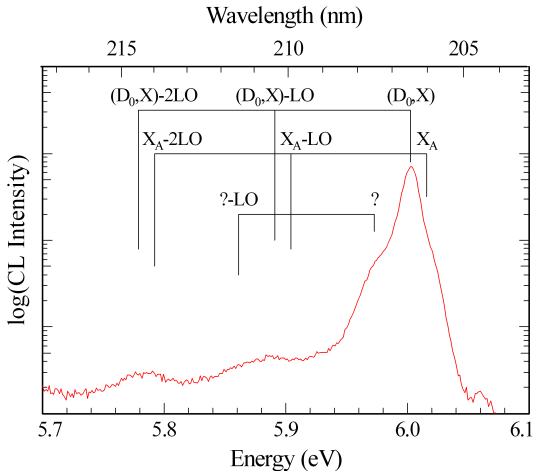

Fig. 3: Low temperature CL spectrum of optimized AlN bulk layer. The FWHM of the CL peak is approx. 10 meV.

(114) reflections, the FWHM increased with increasing Si concentration up to a level of $10^{19}\,\mathrm{cm}^{-3}$ and decreased for higher concentrations (Fig. 5).

Similarly, we found increasing in-plane tensile strain on the AlN:Si layers with increasing Si concentrations up to $10^{19}\,\mathrm{cm}^{-3}$, whereas it decreased for higher concentrations (Fig. 6). A lot of cracks was clearly visible on the surface of such samples under optical microscopy investigations, whereas the samples with Si concentration less than $10^{19}\,\mathrm{cm}^{-3}$ were almost crack free. This behaviour was verified by low temperature CL measurements. Figure 7 demonstrates the red shift of the CL peaks with respect to increasing Si concentrations indicating larger tensile strain, while it was blue shifted for the samples having Si concentration higher than $10^{19}\,\mathrm{cm}^{-3}$. Such an effect of Si incorporation with different concentrations on structural and spectroscopic properties of AlN layers was further evidenced by Raman scattering measurements [14]. Unfortunately, we could not get indications for n–type conductivity in our Si doped AlN layers.

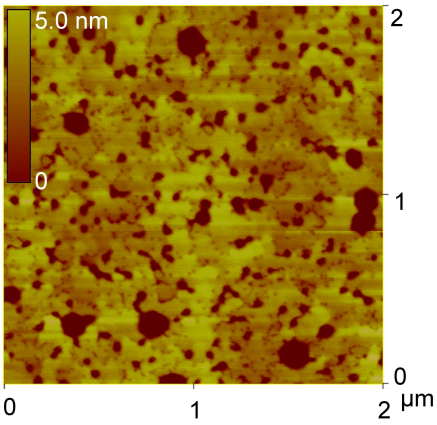

Fig. 4: AFM image of a Si–doped ($9 \cdot 10^{18}\,\mathrm{cm}^{-3}$) AlN layer. A large number of pits are visible.

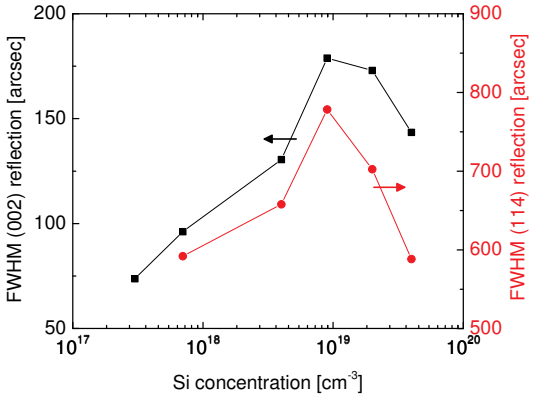

Fig. 5: FWHM of HRXRD for (002) and (114) reflections for different Si concentrations.

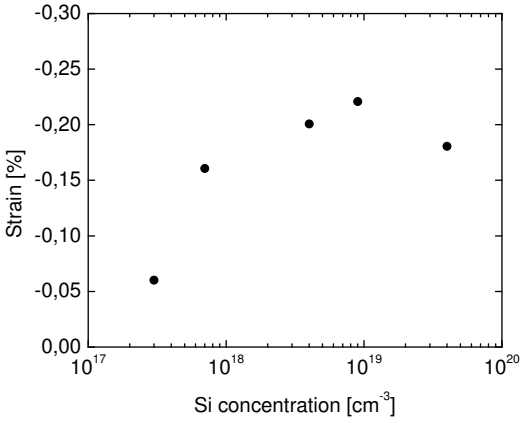

Fig. 6: Strain of Si–doped AlN layers at various Si concentrations determined from the HRXRD rocking curve measurements.

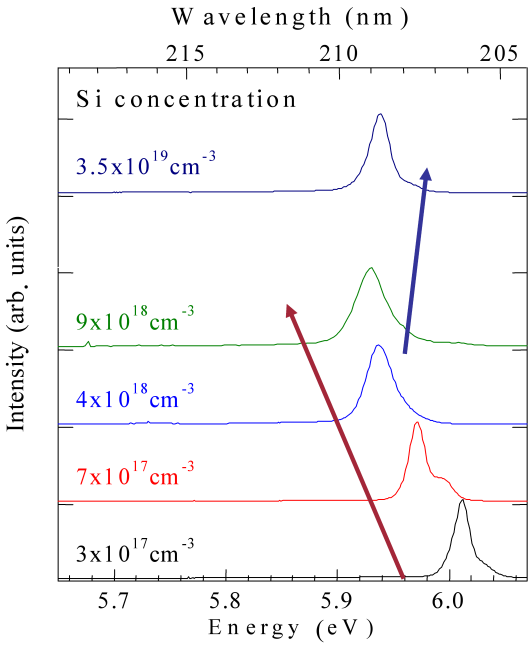

Fig. 7: Red shifting of CL peak of AlN layers till the Si concentration of $10^{19}\,\mathrm{cm}^{-3}$ and blue shifting for higher concentration.

4. Summary

We obtained very high quality AlN layers having rms surface roughness of 0.2 nm, FWHM of HRXRD for (002) and (114) reflections of 59 and 390 arcsec, respectively after optimization of nucleation layer, stage between nucleation and bulk layer, and bulk layer growth where we obtained the best results for a growth temperature of 1190°C. The hexagonal pit density on the surface is determined to be well below $10^5\,\mathrm{cm}^{-2}$. This excellent quality of our AlN layers is further confirmed by low temperature CL spectra with a FWHM

of the donor bound exciton peak of 10 meV. We investigated the effects of Si incorporation on the structural and spectroscopic properties of the AlN layer. It was observed that the surface quality is degraded after Si incorporation. The slight broadening of the (114) reflection of HRXRD measurements can be correlated with the presence of a large number of pits on the surface of Si–doped AlN layers. However, the decrease in FWHM of HRXRD for (002) reflection demonstrates the positive impact of Si on crystal quality. The FWHM of both HRXRD reflections, (002) and (114), increased with increasing Si concentrations up to $10^{19}\,\mathrm{cm}^{-3}$ and decreased for higher concentrations. Furthermore, HRXRD and low temperature CL measurements show increasing in-plane tensile stress up to Si concentrations of $10^{19}\,\mathrm{cm}^{-3}$ and release of such stress by crack formation for higher concentrations.

Acknowledgment

I would like to thank G.M. Prinz, and K. Thonke of the Institute of Semiconductor Physics for CL and Raman measurements; L. Kirste, T. Fuchs, and M. Grimm of Fraunhofer–Institut für Angewandte Festkörperphysik for SIMS measurements. S. Wabra and Hu Wenjie for AFM measurements; J. Hertkorn and P. Brückner for fruitful discussions on epitaxy and system maintenances. This work was financially supported by the Deutsche Forschungsgemeinschaft.

References

[1] C.M. Yang, K. Uehara, S.K. Kim, S. Kameda, H. Nakase, and K. Tsubouchi, "Highly c-axis-oriented AlN film using MOCVD for 5GHz-band FBAR filter", *IEEE Symposium on Ultrasonics*, vol. 1, pp. 170–173, 2003.

[2] R. Lanz, and P. Muralt, "Solidly mounted BAW filters for 8 GHz based on AlN thin films", *IEEE Symposium on Ultrasonics*, vol. 1, pp. 178–181, 2003.

[3] Y. Taniyasu, M. Kasu, and T. Makimoto, "An aluminium nitride light-emitting diode with a wavelength of 210 nanometers", *Nature (London)*, vol. 441, no. 18, pp. 325–328, 2006.

[4] T.M. Katona, T. Margalith, C. Moe, M.C. Schmidt, C. Matt, S. Nakamura, J.S. Speck, S.P. DenBaars, and P. Steven, "Growth and fabrication of short-wavelength UV LEDs", in *Third International Conference on Solid State Lighting*, I.T. Ferguson, N. Narendran, S.P. DenBaars, J.C. Carano (Eds.), Proc. SPIE 5187, pp. 250–259, 2004.

[5] M. Shatalov, Z. Gong, M. Gaevski, S. Wu, W. Sun, V. Adivarahan, and M.A. Khan, "Reliability of AlGaN-based deep UV LEDs on sapphire", *Light-Emitting Diodes: Research, Manufacturing, and Applications*, K.P. Streubel, H.W. Yao, E.F. Schubert (Eds.), Proc. SPIE 6134, pp. 61340P, 2006.

[6] D. Hofstetter, S. Schad, H. Wu, W.J. Schaff, and L.F. Eastman, "GaN/AlN-based quantum-well infrared photodetector for 1.55 m", *Appl. Phys. Lett.*, vol. 83, pp. 572–575, 2003.

[7] I. Waki, C. Kumtornkittikul, Y. Shimogaki, and Y. Nakano, "Shortest intersubband transition wavelength (1.68 µm) achieved in AlN/GaN multiple quantum wells by metalorganic vapor phase epitaxy", *Appl. Phys. Lett.*, vol. 82, pp. 4465–4467, 2002.

[8] S.B. Thapa, C. Kirchner, F. Scholz, G.M. Prinz, K. Thonke, R. Sauer, A. Chuvilin, J. Biskupek, U. Kaiser, and D. Hofstetter, "Structural and spectroscopic properties of AlN layers grown by MOVPE", *J. Crystal Growth*, vol. 298, pp. 383–386, 2007.

[9] B. Kuhn and F. Scholz, "An Oxygen Doped Nucleation Layer for the Growth of High Optical Quality GaN on Sapphire", *physica status solidi (a)*, vol. 188, no. 2, pp. 629–633, 2001.

[10] L. Kirste, T. Fuchs, and M. Grimm; Fraunhofer–Institut für Angewandte Festkörperphysik, Freiburg, Samples Y987,Y989,Y990.

[11] S.B. Thapa, *Annual Report 2005*, Optoelectronics Department, Ulm University.

[12] T. Ive, O. Brandt, H. Kostial, K.J. Friedland, L. Däweritz, and K.H. Ploog "Controlled n-type doping of AlN:Si films grown on 6H-SiC(0001) by plasma-assisted molecular beam epitaxy", *Appl. Phys. Lett.*, vol. 86, pp. 024106, 2005.

[13] V. Lebedev, F.M. Morales, H. Romanus, S. Krischok, G. Ecke, V. Cimalla, M. Himmerlick, T. Stauden, D. Cengher, and O. Ambacher "The role of Si surfactant and donor in molecular-beam epitaxy of AlN", *J. Appl. Phy.*, vol. 98, pp. 093508, 2005.

[14] G.M. Prinz, M. Feneberg, M. Schirra, K. Thonke, R. Sauer, S.B. Thapa, F. Scholz, M. Bickermann, and B. Epelbaum "Optical Spectroscopy of doped and undoped Aluminium Nitride Layers on Sapphire Substrates ", *DGKK-Workshop III-V-Epitaxie*, Ulm, Germany, Dec. 2006